ARMY RESEARCH LABORATORY

Viscoelastic Response of Prestressed Composite Cylinders for Rotating Machinery Applications

by Jerome T. Tzeng

ARL-TR-1590

January 1998

Army Research Laboratory
Aberdeen Proving Ground, MD 21005-5066

ARL-TR-1590 **January 1998**

Viscoelastic Response of Prestressed Composite Cylinders for Rotating Machinery Applications

Jerome T. Tzeng
Weapons and Materials Research Directorate, ARL

Abstract

Energy storage devices such as composite rotors are built with radial precompression to enhance mechanical performance; however, the preload might decrease due to the viscoelastic behavior of materials at elevated temperatures. In this investigation, an analytical solution is developed to study the viscoelastic problem of thick-walled cylinders. The analysis accounts for ply-by-ply variations of properties, fiber orientations, and temperature gradients through the thickness of cylinders. Fiber-reinforced composite materials generally illustrate extreme anisotropy in viscoelastic behavior. The viscoelasticity exists mainly in matrix-dominant properties such as transverse and shear while the fiber-dominant properties behave more like elastic mediums. Accordingly, the viscoelastic characteristics of composite cylinders are quite different from those of isotropic cylinders. Currently, finite-element packages such as ABAQUS, ANSYS, and DYNA3D are not suitable for the viscoelastic analysis of composite cylinders because of the lack of anisotropic viscoelastic elements. The prestress in the hoop-wound fibers, which generates radial compression in the cylinders, might decrease due to Poisson's effect alone from the creep behavior in the transverse properties of composite. The result also shows the effects of layup construction and fiber orientations on the anisotropic behavior of composite cylinders.

Acknowledgment

The author would like to express his gratitude to Dr. Ian McNab of The Institute for Advanced Technology, The University of Texas at Austin, for his support.

INTENTIONALLY LEFT BLANK.

Table of Contents

		Page
	Acknowledgment	iii
	List of Figures	vii
1.	Introduction	1
2.	Viscoelastic Formulation	3
3.	Relaxation of Thermal Stresses	9
4.	Relaxation of Mechanical Stresses	12
5.	Conclusions	20
6.	References	21
	Distribution List	23
	Report Documentation Page	31

INTENTIONALLY LEFT BLANK.

List of Figures

Figure		Page
1.	Cylindrical Coordinate System (r, q, z) of a Laminated Cylinder Containing N Layers	4
2.	Continuity Boundary Conditions of Radial Displacement and Stresses at the Interfaces of Adjacent Layers	8
3.	Time-Dependent Transverse and Shear Compliances at Various Temperatures	9
4.	Radial Displacement Profiles Across the Thickness of the Cylinder at Three Different Instants: $t = 10^{-3}$ min, $t = 10^{4.5}$ min, and $t = 10^{12}$ min	11
5.	Radial Stress Profiles Across the Thickness of the Cylinder at Three Different Instants: $t + 10^{-3}$ min, $t = 10^{4.5}$ min, and $t = 10^{12}$ min	11
6.	Hoop Stress Profiles Across the Thickness of the Cylinder at Three Different Instants: (a) $t = 10^{-3}$ min, (b) $t = 10^{4.5}$ min, and (c) $t = 10^{12}$ min	13
7.	Axial Stress Profiles Across the Thickness of the Cylinder at Three Different Instants: (a) $t = 10^{-3}$ min, (b) $t = 10^{4.5}$ min, and (c) $t = 10^{12}$ min	14
8.	Inplane Shear Stress Profiles Across the Thickness of the Cylinder at Three Different Instants: (a) $t = 10^{-3}$ min, (b) $t = 10^{4.5}$ min, and (c) $t = 10^{12}$ min	15
9.	Precompression at the Interface of a Composite Cylinder and Rigid Mandrel Can Be Achieved by a Press-Fit Process With a Proper Interference	16
10.	Creeping With Time of the Radial Displacement Through the Thickness of a Composite Overwrapped Cylinder	17
11.	Relaxation With Time of Radial Stress Through the Thickness of a Composite Overwrapped Cylinder	17
12.	Creep Compliance of Fibrite 977-2 Epoxy Measured by DMA at a Reference Temperature of 121° C	19
13.	Relaxation of Interference Pressure of a 10-in-Diameter Composite Cylinder at Three Tme Instants	19

INTENTIONALLY LEFT BLANK.

1. Introduction

Composite materials are currently used for highly efficient rotors, as an energy storage device. For these applications, prestresses are built in during fabrication of the cylinders through a press-fit procedure to enhance the mechanical performance. In a high-speed rotor, centrifugal force resulting from the rotation during operation generates tensile stresses in the radial and circumferential directions. Since the composite rotors are primarily reinforced in a circumferential direction, the radial tensile is critical to the ultimate performance of the rotors due to the weakness of radial strength. Accordingly, it is crucial to build and maintain a certain level of radial compression in the rotor prior to operation. Reinforced composite materials are also used for construction of lightweight gun barrels. Composite gun tubes are generally built with a metal liner and a composite overwrap. Because of a thick-walled construction, there is a stress gradient through the thickness of barrels as subjected to propellant pressure. For a gun barrel application, there is a stress gradient through the wall thickness. The stress gradient has to be minimized to achieve the optimal structural performance. Composite gun barrels must be prestressed; therefore, the composite overwrap is in a state of tension to induce compression in the steel liner.

Polymer materials in general behave viscoelastically, which means that creep associated with stress relaxation occurs in a long period of time, especially at elevated temperatures (Ferry 1961). The associated stress relaxation in the composite wall results in loss of the prestresses and potentially leads to structural failures or downgrade in performance. Fiber-reinforced composites with polymer matrix carry the same characteristic, but behave more complicatedly due to anisotropy. For carbon-fiber composite, fiber-dominant properties such as modulus in the fiber direction are sort of elastic. The viscoelasticity exists mainly in matrix-dominant properties such as transverse moduli and shear properties. Because of the extreme anisotropic characteristic, a composite cylinder will behave quite differently from one built with isotropic materials. The objective of this investigation is to develop an analytical method to study the viscoelastic behavior of the thick-walled composite cylinders. The analysis can be applied to the design of flywheel machinery and overwrapped composite gun tubes.

To date, activities in the research of viscoelasticity have mainly concerned isotropic materials included in the studies by Muki and Sternberg (1961), Schapery (1964), Williams (1964), and Christensen (1982). These basic theories of viscoelasticity were then extended to the area of heterogeneous and anisotropic materials for a variety of applications. Hashin (1965) used the effective relaxation moduli and creep compliances to define the macroscopic viscoelastic behavior of linear viscoelastic heterogeneous media and its implementation in viscoelastic modeling. The general formulation of linear viscoelastic boundary value problems of composite materials, including the thermal viscoelastic problems for thermorheologically simple materials and the applications of the correspondence principle, were examined by Schapery (1967). Rogers and Lee (1964) investigated the viscoelastic behavior of an isotropic cylinder.

In the following research, the linear quasi-static viscoelastic behavior of a thick laminated composite cylinder with an elevated temperature change is studied. The analysis accounts for ply-by-ply variation of properties, temperature changes, and fiber orientations. The thick cylinder is assumed to be in the absence of thermomechanical coupling and to be in the state of generalized plane strain, such that all the stress and strain components are independent of the axial coordinate (Tzeng and Chien 1994). Moreover, due to the nature of axisymmetry, all the stress and strain components are also independent of the circumferential coordinate. The mechanical responses of this thick composite cylinder will, therefore, only have to satisfy the governing equation in the radial direction. Invoking the Boltzmann superposition integral for the complete spectrum of increments of anisotropic material constants with respect to time, the thermoviscoelastic constitutive relations of the anisotropic composite cylinder can be derived in integral forms. Since the thick composite cylinder is subjected to a constant elevated temperature change, and boundary conditions are all independent of time, formulations of the linear thermal viscoelastic problem can have forms identical to those of the corresponding linear thermoelastic problem by taking advantage of the elastic-viscoelastic correspondence principle. In other words, all of these integral constitutive equations reduce to algebraic relations that are very similar to those developed for thermoelastic media when they are Laplace transformed by means of the rule for convolution integrals. The thermoelastic analysis can thus be used to derive the transformed thermal viscoelastic solutions in the frequency domain.

2. Viscoelastic Formulation

Consider a filament-wound axisymmetric thick composite cylinder consisting of N layers with the axial coordinate z, the radial coordinate r, and the circumferential coordinate θ, as shown in Figure 1. This composite cylinder has the inner radius a, the outer radius b, and the length L. The Boltzmann superposition integral of a stress σ_{ij} (i, j = 1, 2, 3) and strain ϵ_{ij} (i, j = 1, 2, 3) relation for an isothermal viscoelastic problem with a constant temperature increase ΔT and the thermal expansion coefficient α_{kl} is

$$\sigma_{ij}(t) = \int_0^t C_{ij}^{kl}(T, t-\tau) \frac{\partial \epsilon_{kl}(\tau)}{\partial \tau} d\tau - \beta_{ij}(T,t)\Delta T , \tag{1}$$

where $C_{ij}^{kl}(T,t)$ is the relaxation modulus dependent on temperature T and time t,

$$C_{ij}^{kl}(T(t),t) = C_{ij}^{kl}(T_0, \lambda(t))$$
$$\lambda(t) = \frac{t}{a_T(T(t))} .$$

Here, T_0 is the base temperature, and a_T is the temperature-shift factor. $\beta_{ij}(T,t)$ is given by $B_{ij}(T,t) = C_{ij}^{kl}(T,t) \cdot \alpha_{kl}$. It is often desirable to use the inverse form of the constitutive relation (1),

$$\epsilon_{ij}(t) = \int_0^t A_{ij}^{kl}(T, t - \tau) \frac{\partial \sigma_{kl}(\tau)}{\partial \tau} d\tau + \psi_{ij}(T,t)\Delta T , \tag{2}$$

where $\psi_{ij}(T,t)$ is the tensor product of the creep compliance $A_{ij}^{kl}(T,t)$ and the thermal creep coefficient ϕ_{kl}. Since the elevated temperature change ΔT is constant above some reference value in time, the relaxation moduli and creep compliances are evaluated at that reference temperature regardless of whether or not the material is thermorheologically simple by employing the temperature-shift factor.

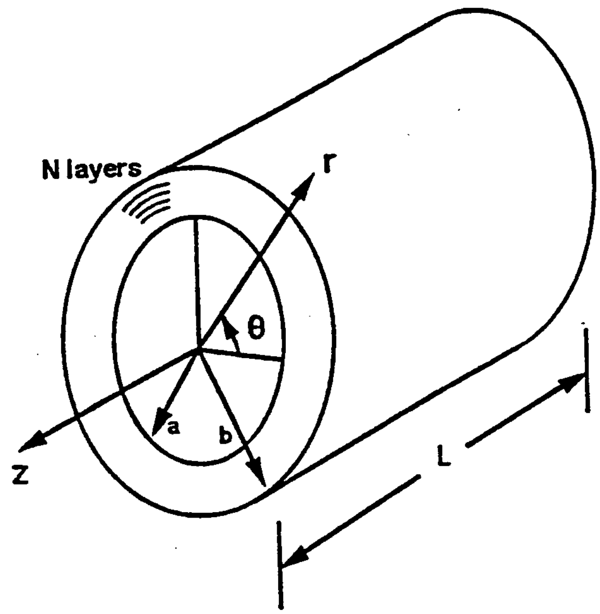

Figure 1. Continuity Cylindrical Coordinate System (r, q, z) of a Laminated Cylinder Containing N Layers.

The Laplace transform of a function f(t) is defined as

$$\bar{f} = \bar{f}(s) = \int_0^\infty e^{-st} f(t)\,dt\,, \tag{3}$$

where s is the Laplace transform variable. Applying (3) with the convolution rule to (1) and (2) reduces the integral constitutive equations to the following algebraic relations:

$$\bar{\sigma}_{ij} = \tilde{C}_{ij}^{kl}\,\tilde{\epsilon}_{kl} - \tilde{\beta}_{ij}\frac{\Delta T}{s}\,, \tag{4}$$

and the inverse form

$$\tilde{\epsilon}_{ij} = \tilde{A}_{ij}^{kl}\,\bar{\sigma}_{ij} + \tilde{\psi}_{ij}\frac{\Delta T}{s}\,, \tag{5}$$

respectively, where

$$\tilde{C}_{ij}^{kl} = s\bar{C}_{ij}^{kl},\ \tilde{A}_{ij}^{kl} = s\bar{A}_{ij}^{kl},\ \tilde{\alpha}_{ij} = s\bar{\alpha}_{ij}, \tilde{\phi}_{ij} = s\bar{\phi}_{ij}, \tilde{\beta}_{kl} = \tilde{C}_{ij}^{kl}\cdot\tilde{\alpha}_{ij}, \text{ and } \tilde{\psi}_{kl} = \tilde{A}_{ij}^{kl}\cdot\tilde{\phi}_{ij}.$$

Furthermore, it can be shown that $\left[\tilde{A}_{ij}^{kl}\right] = \left[\tilde{C}_{ij}^{kl}\right]^{-1}$.

Consider a corresponding thermoelastic problem with the transformed displacement components $\bar{u}$, $\bar{v}$, and $\bar{w}$ in the axial direction, the circumferential direction, and the radial direction, respectively, in each layer. The axisymmetric character of the thick composite cylinder along with the assumption of the state of generalized plane strain leads to a simplified displacement field, which reflects the circumferential independence and only-radial dependence of $\bar{w}$,

$$\begin{aligned} \bar{u}(r,\theta,z) &= \bar{u}(r,z) \\ \bar{v}(r,\theta,z) &= \bar{v}(r,z) \\ \bar{w}(r,\theta,z) &= \bar{w}(r). \end{aligned} \tag{6}$$

Substituting these transformed displacement components into the strain-displacement relations and invoking the compatibility conditions, one can derive explicit forms of $\bar{u}$ and $\bar{v}$. Since each layer of the thick laminated cylinder is cylindrically monoclinic in reference to the global coordinates, there is no coupling between transverse shears and other deformations. Accordingly, the vanishing shear traction boundary conditions and interface continuity conditions generate zero out-of-plane shear tractions and shear strains for each layer. Moreover, owing to the absence of torsional deformation, the transformed displacement components $\bar{u}$ and $\bar{v}$ become

$$\begin{aligned} \bar{u} &= \bar{\epsilon}^0 z \\ \bar{v} &= 0, \end{aligned} \tag{7}$$

where the constant quantity $\bar{\epsilon}^0$ has the physical interpretation of transformed axial strain of a layer. In fact, $\bar{\epsilon}^0$, according to the present formulation, also represents the transformed axial strain of the entire composite cylinder. The calculation of $\bar{\epsilon}^0$ requires the knowledge of end boundary conditions and will be given later. Likewise, solving for $\bar{w}(r)$ requires the information of transformed strain components, the constitutive equations, as well as the equilibrium equations.

The previously transformed displacement field gives the transformed strain components in cylindrical coordinates

$$
\begin{aligned}
\bar{\epsilon}_{rr} &= \frac{d\bar{w}(r)}{dr} \\
\bar{\epsilon}_{\theta\theta} &= \frac{\bar{w}(r)}{r} \\
\bar{\epsilon}_{zz} &= \frac{d\bar{u}}{dz} = \bar{\epsilon}^{0} \\
\bar{\epsilon}_{\theta r} &= \bar{\epsilon}_{zr} = \bar{\epsilon}_{z} = 0 \,.
\end{aligned}
\tag{8}
$$

The unabridged form of the constitutive equation (4) for each layer in cylindrical coordinates with the radial coordinate r normal to the plane of symmetry is expressed as

$$
\begin{Bmatrix} \bar{\sigma}_{zz} \\ \bar{\sigma}_{\theta\theta} \\ \bar{\sigma}_{rr} \\ \bar{\sigma}_{\theta r} \\ \bar{\sigma}_{zr} \\ \bar{\sigma}_{z\theta} \end{Bmatrix} = \begin{bmatrix} \tilde{C}_{11} & \tilde{C}_{12} & \tilde{C}_{13} & 0 & 0 & \tilde{C}_{16} \\ \tilde{C}_{12} & \tilde{C}_{22} & \tilde{C}_{23} & 0 & 0 & \tilde{C}_{26} \\ \tilde{C}_{13} & \tilde{C}_{23} & \tilde{C}_{33} & 0 & 0 & \tilde{C}_{36} \\ 0 & 0 & 0 & \tilde{C}_{44} & \tilde{C}_{45} & 0 \\ 0 & 0 & 0 & \tilde{C}_{45} & \tilde{C}_{55} & 0 \\ \tilde{C}_{16} & \tilde{C}_{26} & \tilde{C}_{36} & 0 & 0 & \tilde{C}_{66} \end{bmatrix} \begin{Bmatrix} \bar{\epsilon}_{zz} \\ \bar{\epsilon}_{\theta\theta} \\ \bar{\epsilon}_{rr} \\ \bar{\epsilon}_{\theta r} \\ \bar{\epsilon}_{zr} \\ \bar{\epsilon}_{z\theta} \end{Bmatrix} - \frac{\Delta T}{s} \begin{Bmatrix} \tilde{B}_{zz} \\ \tilde{B}_{\theta\theta} \\ \tilde{B}_{rr} \\ 0 \\ 0 \\ \tilde{B}_{z\theta} \end{Bmatrix} . \tag{9}
$$

Furthermore, from the previous discussions, it can be shown that two of the three equilibrium equations are satisfied automatically. The only nontrivial equilibrium equation is the one in the radial direction:

$$
\frac{\partial \bar{\sigma}_{rr}}{\partial r} + \frac{\bar{\sigma}_{rr} - \bar{\sigma}_{\theta\theta}}{r} = 0 \,. \tag{10}
$$

Substituting (6), (7), and (8) into (9), the transformed stress components $\bar{\sigma}_{rr}$ and $\bar{\sigma}_{\theta\theta}$ are obtained in terms of the transformed radial displacement $\bar{w}$. Incorporating the resulting $\bar{\sigma}_{rr}$ and $\bar{\sigma}_{\theta\theta}$ functions with (10) gives a nonhomogeneous Euler differential equation of $\bar{w}$ for a layer

$$
r^2 \frac{d^2 \bar{w}}{dr^2} + r \frac{d\bar{w}}{dr} - \tilde{\lambda}^2 \bar{w} = \frac{r}{\tilde{C}_{33}} \left[\frac{\Delta T}{s} (\tilde{B}_{rr} - \tilde{B}_{\theta\theta}) - (\tilde{C}_{13} - \tilde{C}_{12}) \bar{\epsilon}^{o} \right], \tag{11}
$$

where

$$\tilde{\lambda}^2 = \frac{\tilde{C}_{22}}{\tilde{C}_{33}} . \tag{12}$$

Solving (11) for $\bar{w}$ yields

$$\bar{w} = \bar{A}_1 r^{\tilde{\lambda}} + \bar{A}_2 r^{-\tilde{\lambda}} + \tilde{w}_p , \tag{13}$$

where

$$\begin{aligned} \tilde{w}_p &= \tilde{f}_1 \bar{\epsilon}^o r + \tilde{f}_3 r \\ \tilde{f}_1 &= \frac{\tilde{C}_{12} - \tilde{C}_{13}}{\tilde{C}_{33} - \tilde{C}_{22}} \\ \tilde{f}_3 &= \frac{\tilde{S}}{\tilde{C}_{33} - C_{22}} \\ \tilde{S} &= \frac{\Delta T}{s}\left[\tilde{B}_{rr} - \tilde{B}_{\theta\theta}\right] , \end{aligned} \tag{14}$$

and $\bar{A}_1$ and $\bar{A}_2$ are coefficients to be determined from boundary and continuity conditions.

Finally, it is understood that the initial condition of the original thermoviscoelastic problem is displacement-free state of rest. The boundary conditions are of free tractions and, hence, of free transformed tractions on both inner and outer circular surfaces:

$$\bar{\sigma}_{rr} = \bar{\sigma}_{\theta r} = \bar{\sigma}_{zr} = 0 \quad \text{at} \quad r = a, b . \tag{15}$$

On both end surfaces, stress resultants are zero:

$$\sum_{k=1}^{N} \int_{r_i}^{r_o} \bar{\sigma}_{zz} r dr = \bar{\sigma}_{zr} = \bar{\sigma}_{z\theta} = 0 \quad \text{at} \quad z = 0, L , \tag{16}$$

where r_i and r_o are inner and outer radii, respectively, of the kth layer. The continuity conditions at each interface between two adjacent layers require continuous radial traction and continuous radial displacement at any instant as shown in Figure 2. Thus, when written in the transformed form, they become

$$\bar{\sigma}^{(k)}_{rr,o} - \bar{\sigma}^{(k+1)}_{rr,i} = 0 \tag{17}$$

and

$$\bar{w}^{(k)}_{,o} = \bar{w}^{(k+1)}_{,i}, \tag{18}$$

where $k = 1, \cdots, N - 1$, and subscripts i and o denote inner and outer surfaces, respectively.

Accordingly, the formulation accounts for ply-by-ply variations of material properties and temperature change. The matrix form numerical solution procedure with parallel computing techniques resolved the complexity and time-consuming calculation procedures in a Laplace transform of a multilayered composite cylinder (Chien and Tzeng 1995).

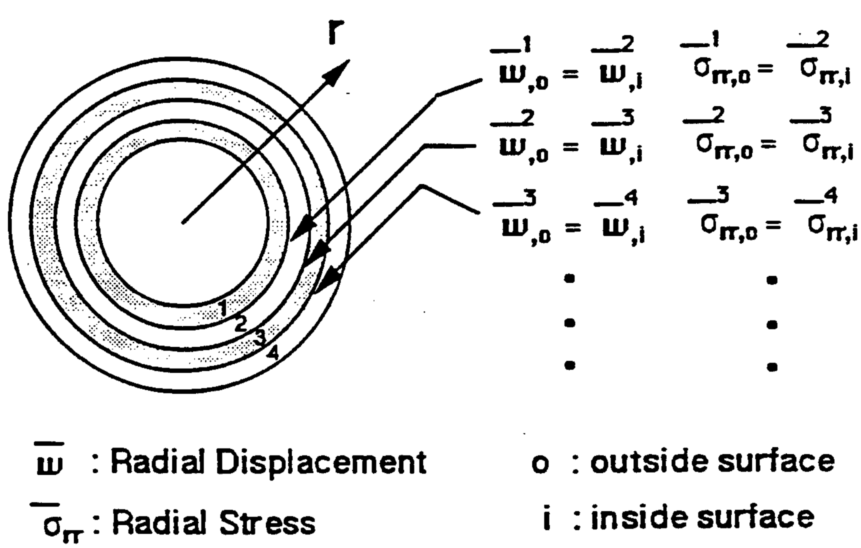

Figure 2. Continuity Boundary Conditions of Radial Displacement and Stresses at the Interfaces of Adjacent Layers.

3. Relaxation of Thermal Stresses

The time-dependent thermal viscoelastic behavior of a 100-layer AS-4/3502 graphite epoxy composite cylinder subjected to a temperature increase $\Delta T = 150°$ C is examined. The composite cylinder has an inner radius a = 3.5 in, an outer radius b = 4.1 in, and a thickness of each layer $h = 6.0 \cdot 10^{-3}$ in. Stacking sequence is given as $[0/30/60/90]_{25}$ from inside out with the 0° direction coinciding with the axis of the cylinder. The creep properties of AS-4/3502 graphite epoxy and AS-4/PEEK thermoplastic laminate with a fiber volume fraction of 0.67 were investigated at different temperatures by Kim and Hartness (1987). Figure 3 shows the transverse and shear compliance of the composite at various temperatures. Increase of compliance with time due to creep behaviors of material was found at elevated temperatures.

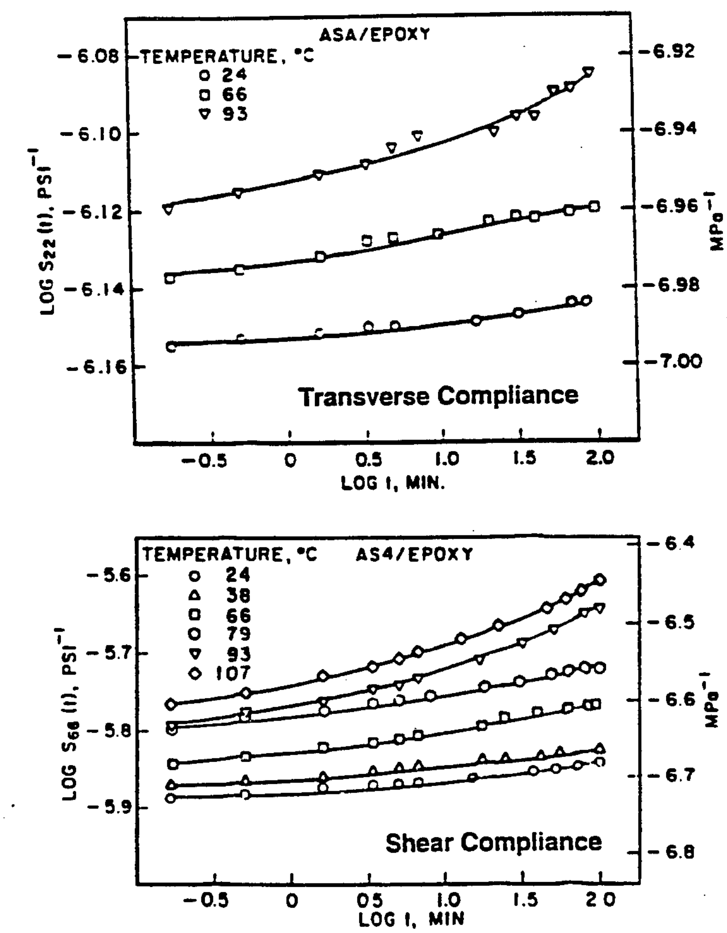

Figure 3. Time-Dependent Transverse and Shear Compliances at Various Temperatures (Kim and Hartness 1987).

In this study, the least-squares curve fitting was used to express the creep compliances from the original AS-4/3502 data at T = 150° C in a power law form

$$S_{22}(t) = \left[1.7051\ (t)^{0.1954} + 1\right] S_{22}^{0} \tag{19}$$

and

$$S_{66}(t) = \left[11.3076\ (t)^{0.2771} + 1\right] S_{66}^{0}, \tag{20}$$

where

$$S_{22}^{0} = 7.5328 \cdot 10^{-7}/\text{psi}$$

$$S_{66}^{0} = 1.3834 \cdot 10^{-6}/\text{psi}.$$

The compliance in the fiber direction, $S_{11} = 5.9 \cdot 10^{-8}$/psi, and Poisson's ratios, $\nu_{12} = \nu_{13} = 0.3$, $\nu_{23} = 0.36$, are assumed to be time independent. Thermal expansion coefficients of the composites in three principal directions are $\alpha_{11} = -0.5 \cdot 10^{-6}/°C$ and $\alpha_{22} = \alpha_{33} = 40.0 \cdot 10^{-6}/°C$, where the negative value indicates shrinkage with temperature increase.

Figures 4 and 5 show radial displacement and radial stress profiles across the thickness of the cylinder at three instants, $t = 10^{-3}$ min, $t = 10^{4.5}$ min, and $t = 10^{12}$ min, respectively. The radial tractions and displacements satisfied the continuity conditions at the interfaces of layers at all instants. The "saw" shaped radial stress distribution results from the discontinuity of material properties and various fiber orientations. The radial displacement, w(t), reaches a steady state at $t = 10^{12}$ min due to a long-term creep behavior. The radial displacement of most layers reaches a constant value, except at the innermost and outermost portions of the cylinder. The free traction boundary at the surface of cylinders causes the gradients in the radial displacements. A similar phenomena is also observed in the radial stresses showing a constant level of stress distribution in the inner portion of cylinder away from boundary layers at $t = 10^{12}$ min. This long-term creep characteristic reflects the proposed power law form, (19) and (20), of the creep compliances.

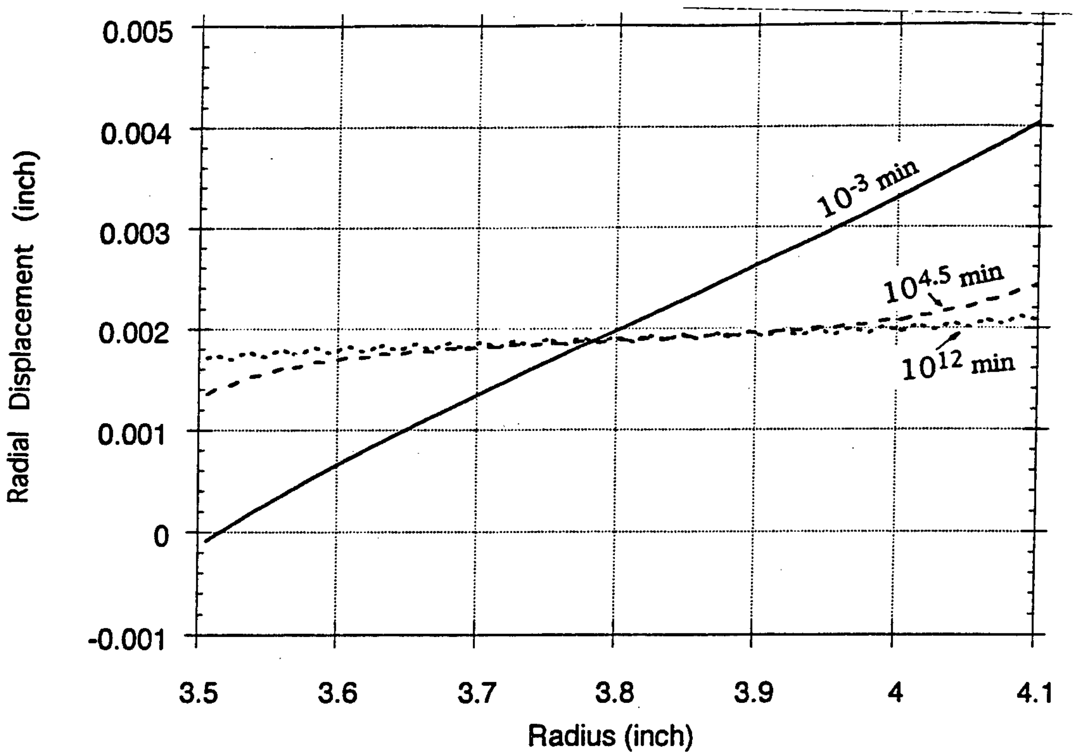

Figure 4. Radial Displacement Profiles Across the Thickness of the Cylinder at Three Different Instants: $t = 10^{-3}$ min, $t = 10^{4.5}$ min, and $t = 10^{12}$ min.

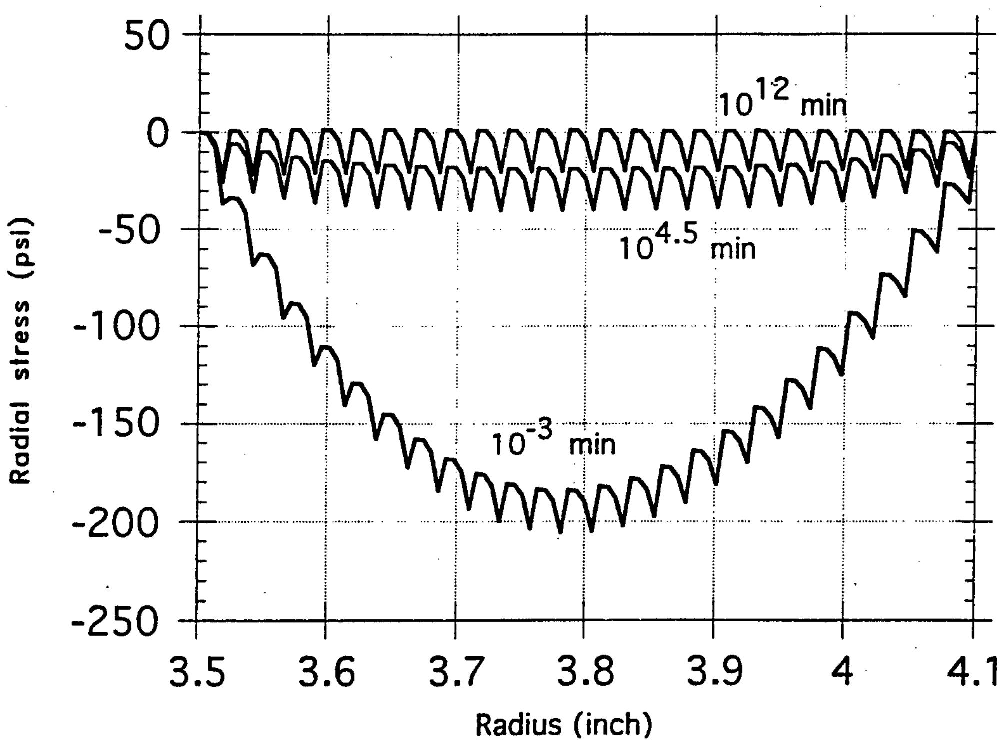

Figure 5. Radial Stress Profiles Across the Thickness of the Cylinder at Three Different Instants: $t = 10^{-3}$ min, $t = 10^{4.5}$ min, and $t = 10^{12}$ min.

The hoop stress, $\sigma_{\theta\theta}(t)$ through the thickness of the cylinder, is illustrated at three instants in Figures 6(a), 6(b), and 6(c), respectively. There exist two distinct values (discontinuity) of $\sigma_{\theta\theta}(t)$ across each interface of two adjacent layers due to the various fiber orientations through the thickness. There is a trend showing the creep behavior of the hoop stress profiles from $t = 10^{-3}$ min to $t = 10^{12}$ min. The hoop stresses in 60° and 90° layers show a fairly steep gradient across the cylinder thickness initially. However, the gradient gradually disappears as time approaches infinity. Likewise, Figures 7(a), 7(b), and 7(c) present the axial stress $\sigma_{zz}(t)$ profiles in the radial direction at the three specified instants, respectively. These figures exhibit similar creep and stress relaxation behaviors as those of hoop stresses $\sigma_{\theta\theta}(t)$. However, the axial stresses in 30° and 60° layers show an increase outwardly from the inside of the cylinder in the early stage. Figures 8(a), 8(b), and 8(c) are the inplane shear stresses $\sigma_{z\theta}(t)$ through the thickness of the cylinder at the three specified instants, respectively. The inplane shear stresses of 0° and 90° layers vanish in the entire time history due to generalized plane strain assumption. A drastic change occurs in the 30° and 60° layers, resulting from the combined effects of Poisson's ratio and creep characteristics of materials.

4. Relaxation of Mechanical Stresses

In the following study, a calculation was performed to simulate a composite cylinder pressed fit on a rigid steel mandrel as shown in a schematic in Figure 9. The 0.6-in-thick composite cylinder has a layup construction of $[90/90/90/0]_{25}$, 75% in hoop and 25% in axial direction. The contact pressure is 1,000 psi at the interface of composite and mandrel, which results from the initial interference. The assembly is then heated and held at 93° C constantly for creep study. In modeling of the experiment, the inner radius of the composite overwrap was held constantly to allow creep and stress relaxation of the cylinder occurring at 93° C. The AS-4/epoxy composite material properties were obtained from Kim and Hartness (1987). A power equation was obtained by a least-square curve-fit technique as follows (Tzeng 1997):

$$S_{22}(t) = 7.553 * 10^{-7} (t)^{0.0175} \tag{21}$$

and

$$S_{66}(t) = 1.383 * 10^{-6} (t)^{0.06} . \tag{22}$$

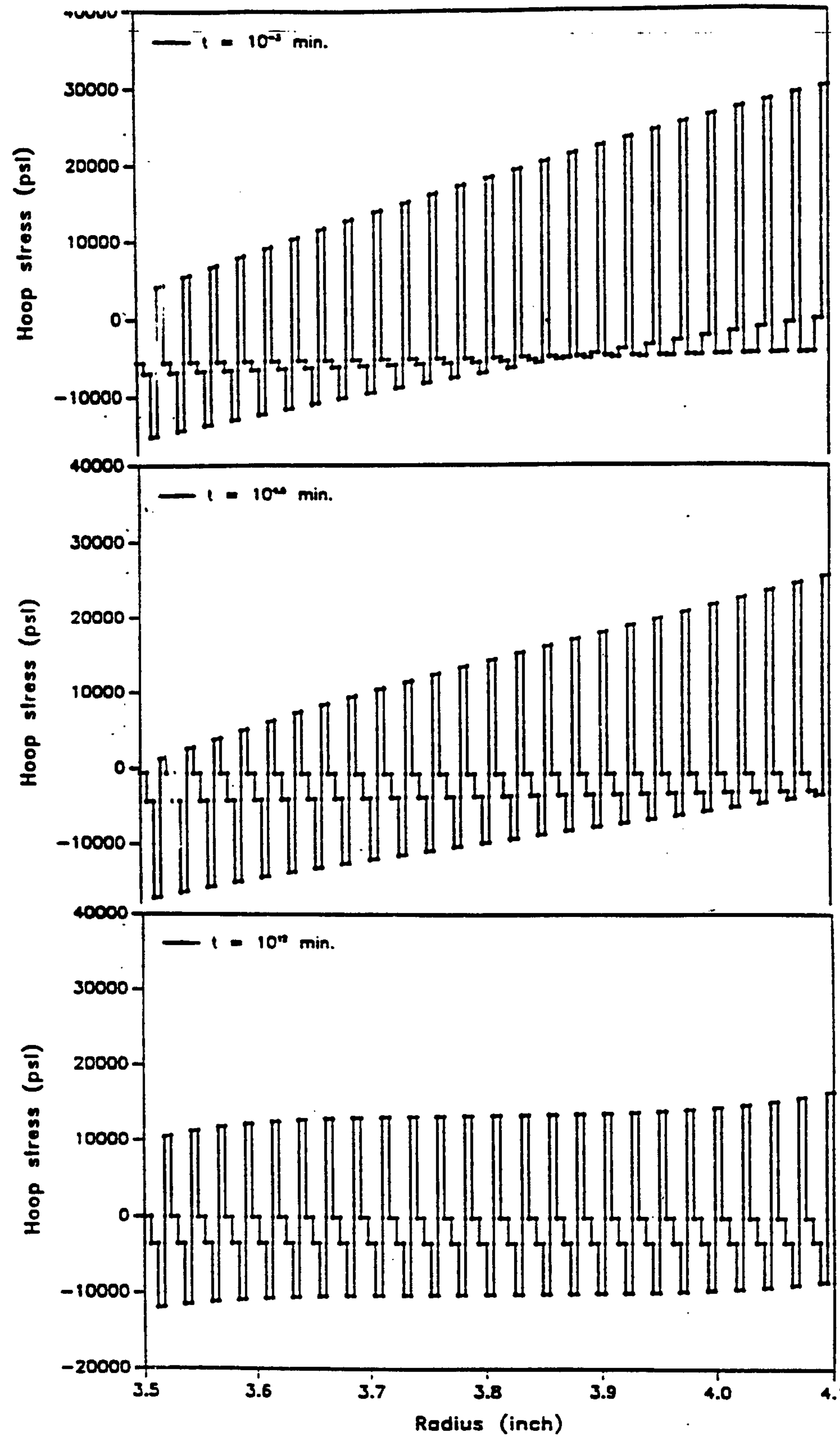

Figure 6. Hoop Stress Profiles Across the Thickness of the Cylinder at Three Different Instants: (a) $t = 10^{-3}$ min, (b) $t = 10^{4.5}$ min, and (c) $t = 10^{12}$ min.

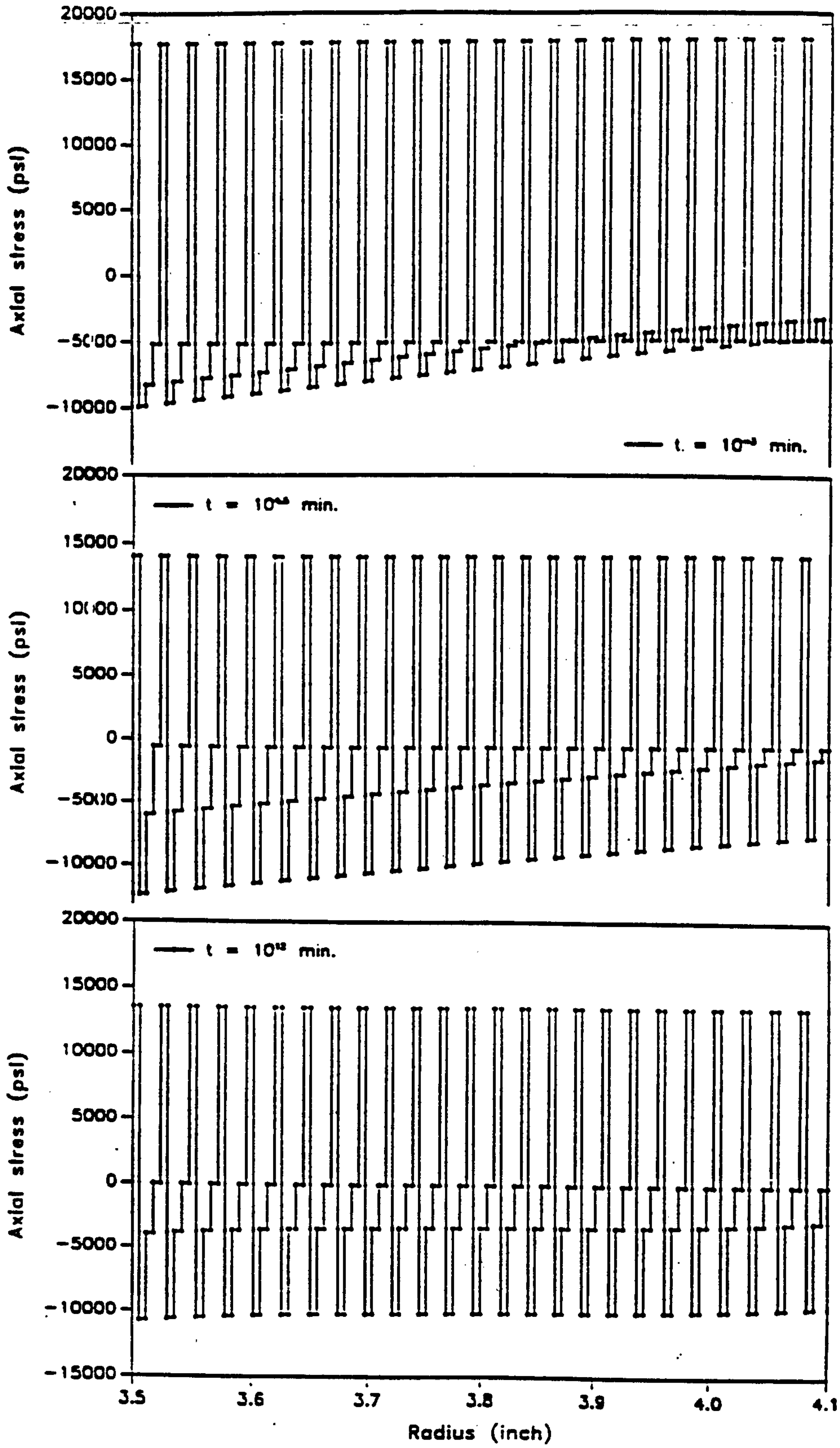

Figure 7. Axial Stress Profiles Across the Thickness of the Cylinder at Three Different Instants: (a) $t = 10^{-3}$ min, (b) $t = 10^{4.5}$ min, and (c) $t = 10^{12}$ min.

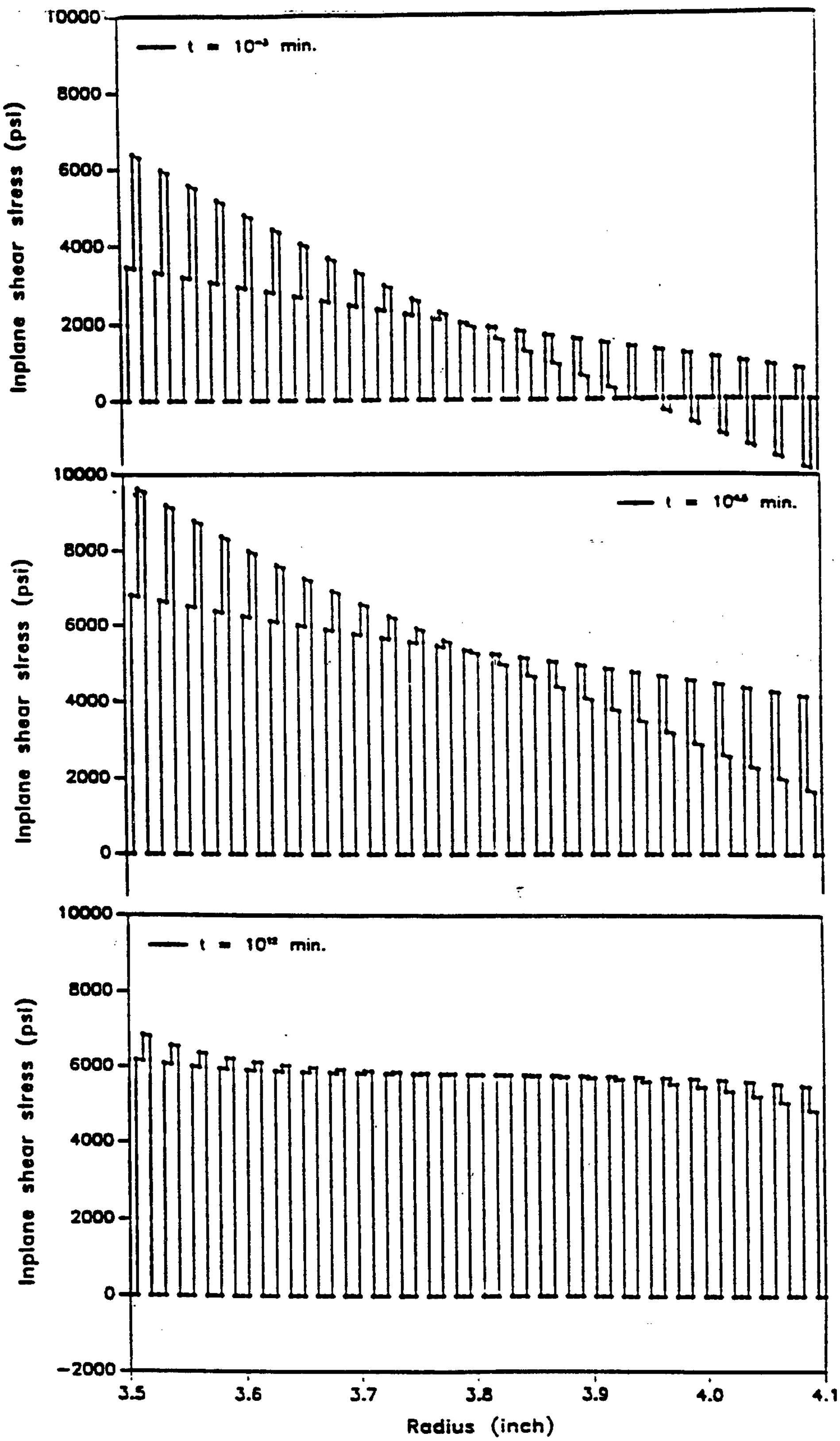

Figure 8. Inplane Shear Stress Profiles Across the Thickness of the Cylinder at Three Different Instants: (a) $t = 10^{-3}$ min, (b) $t = 10^{4.5}$ min, and (c) $t = 10^{12}$ min.

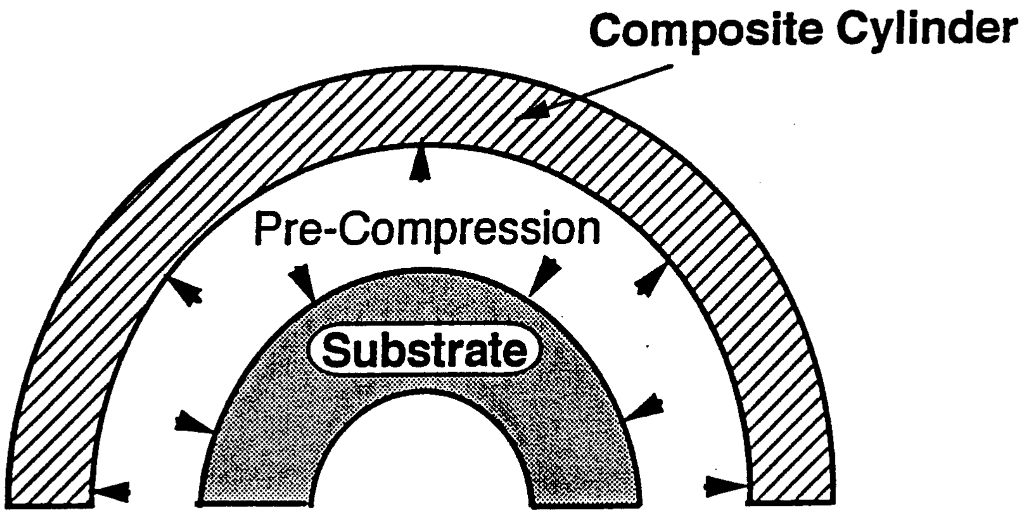

Figure 9. Precompression at the Interface of a Composite Cylinder and Rigid Mandrel Can Be Achieved By a Press-Fit Process With a Proper Interference.

The transverse and shear compliances are in a unit of 1/psi. The compliance in the fiber direction is also assumed to be elastic, as discussed in the previous section.

Figures 10 and 11 illustrate the creep behavior of radial displacement and relaxation of radial stresses as a function of time, respectively. As shown in the plots, a significant loss of preload was in the composite cylinder constructed with this specific material and layup, subjected to an elevated temperature. Tests have been performed using similar basis graphite/epoxy composite materials, and about 20% of preload was lost in a few weeks at elevated temperatures. In general, the rate of loss of preload increases as the temperature increases. The stress relaxation in hoop-wound fiber layers results mainly from Poisson's effects of creep in the transverse direction since the properties are assumed to be elastic in the fiber direction. The stresses will not

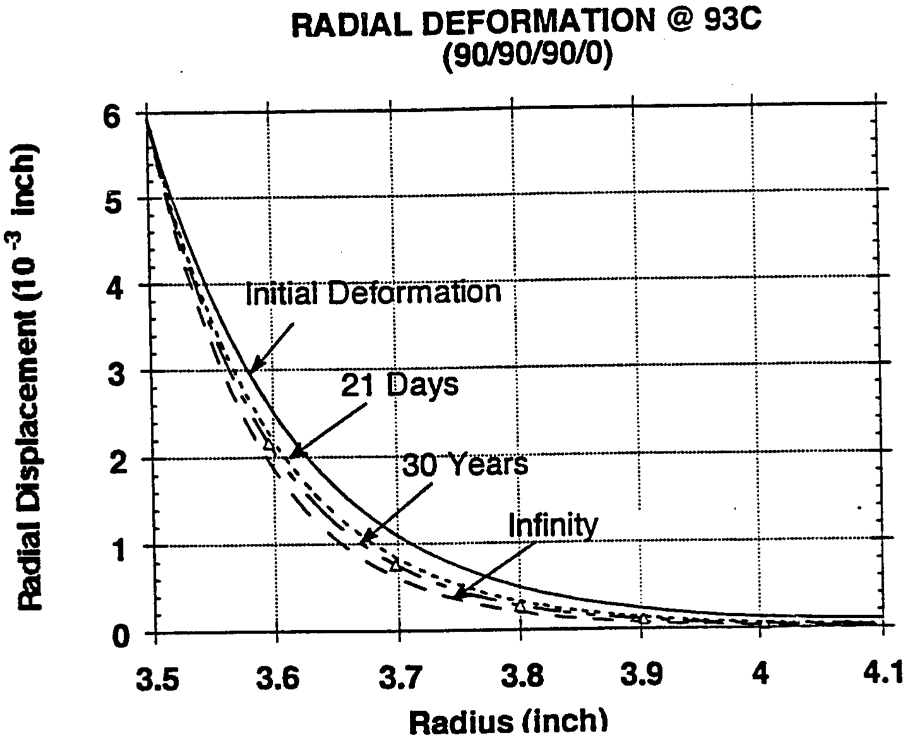

Figure 10. Creeping With Time of the Radial Displacement Through the Thickness of a Composite Overwrapped Cylinder.

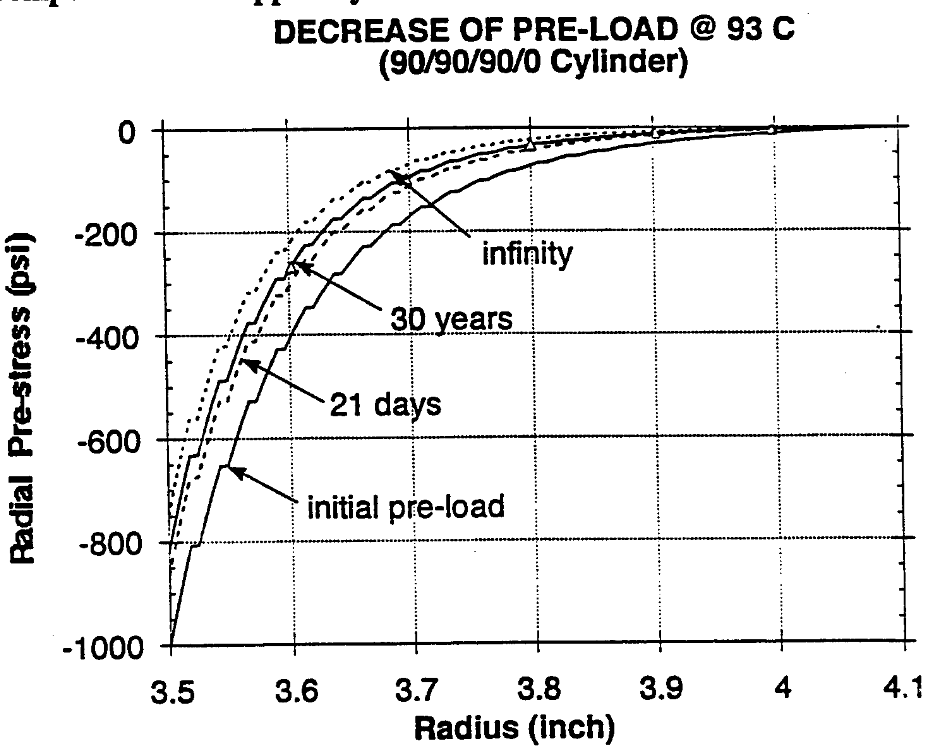

Figure 11. Relaxation With Time of Radial Stress Through the Thickness of a Composite Overwrapped Cylinder.

diminish completely due to elastic properties in the fiber direction. However, the reduction and redistribution of hoop stresses will cause a decrease of the radial compression in the cylinders in a long period. As the radial displacement approaches a uniform state through the thickness, the radial stress will diminish completely, depending upon the material properties and temperatures.

The viscoelastic properties are commonly not available for most composite materials. There is a need to develop a simple and accurate estimation of the viscoelastic properties of composite material for the analysis. This is especially important from an application point of view since there are numerous composite systems available through a combination of matrix and fiber. The following approach is proposed to provide a proper method of material selection based on creep and stress relaxation consideration. The creep compliance of matrix alone can be measured using dynamic mechanical analysis (DMA). Figure 12 shows the measured data of ICI/Fibrite 977-2 resin at a reference temperature of 121° C. The data can then be curve-fit with a time-dependent function as follows:

$$S(t) = S_o \times (t)^{0.04} \tag{23}$$

The expression basically represents the time dependency of the matrix material of composite material. Since the viscoelastic behavior of composite material is mainly dominated by the matrix, it is reasonable to assume the transverse and shear properties of graphite/epoxy (977-2 resin) composite following the power law as equation (23). The elastic properties that are generally available can then be substituted into the expression as the term "S_o" to obtain the viscoelastic properties for the specific composite system. The proposed approach can significantly reduce engineering efforts in material testing if the approximated properties can be applied to the viscoelastic analysis resulting in good agreement with experiment.

In the following study, a cylinder analysis was performed and compared to experimental data. A cylinder with an inner diameter of 10.0 in and a thickness of 1.2 in was fabricated from graphite/epoxy (Im7/977-2) composite material. The laminated cylinder has a ply construction of

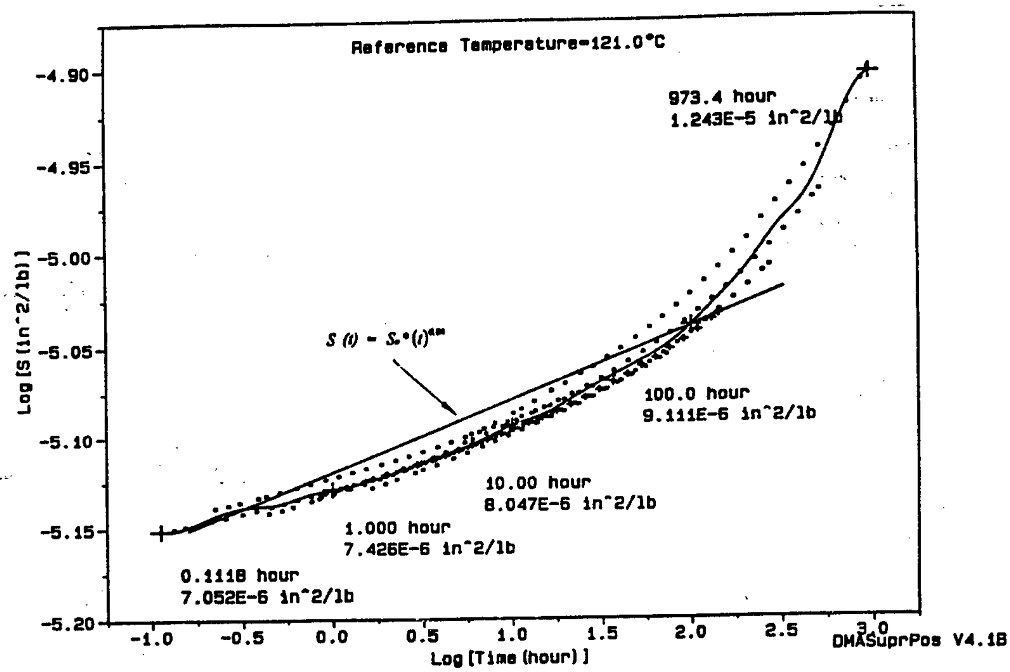

Figure 12. Creep Compliance of Fibrite 977-2 Epoxy Measured by DMA at a Reference Temperature of 121° C (Raw Data Are Provided by CEM, University of Texas at Austin).

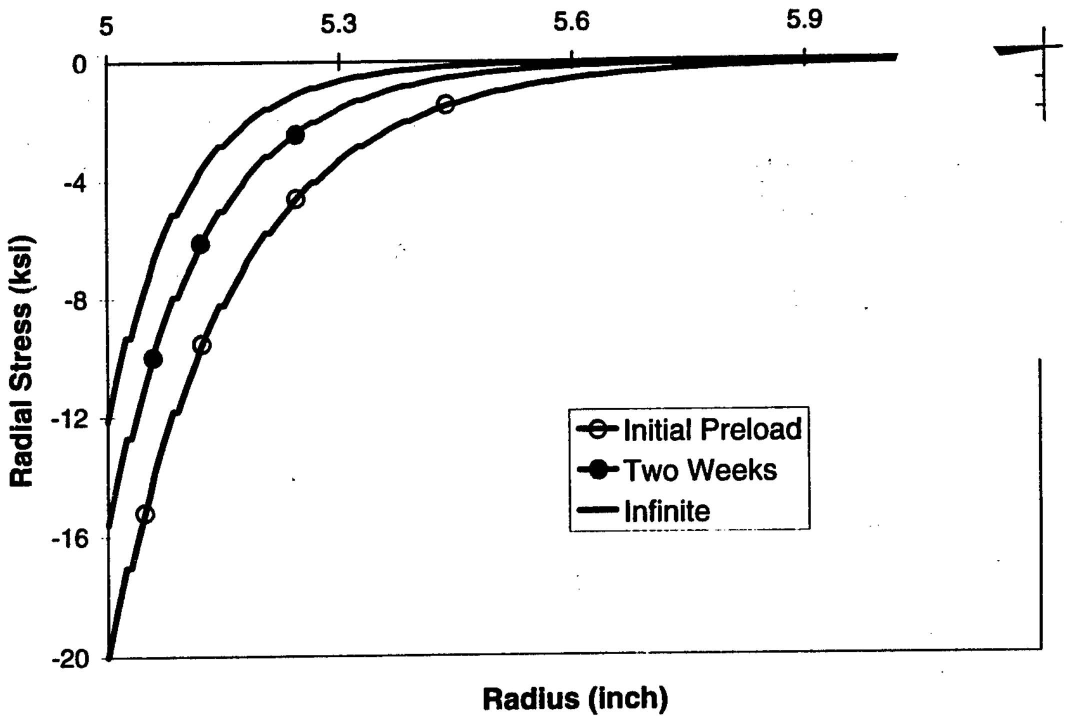

Figure 13. Relaxation of Interference Pressure of a 10-in-Diameter Composite Cylinder at Three Time Instants.

an interference pressure of 20 ksi. The entire assembly is then kept in an oven at 121° C. The hoop strain at the inner radius of the mandrel is monitored, which provides a measure of the preload variation. A loss of preload was found to be 18% in about 14 days. The result of analysis is shown in Figure 13, which indicates a fairly good agreement. Although the validation is limited to a single experiment so far, the correlation does provide confidence of implementation of the proposed approach.

5. Conclusions

An analysis has been developed to study the thermal viscoelastic behavior of thick-walled laminated composite cylinders with ply-by-ply variation of anisotropic viscoelastic properties. The relaxation of stresses and creep behaviors is properly determined in a cylinder subjected to a uniform temperature change. The extreme anisotropy of the viscoelastic behavior of composites results in very interesting as well as important long-term characteristics of cylinders, which cannot be modeled using currently available finite-element codes. Creep and stress relaxation exists in the fiber direction even though the fiber-dominant properties are elastic. This is mainly due to the contribution of the Poisson's effects of viscoelastic transverse and shear properties. Furthermore, the analysis is extended to study the viscoelastic behavior of composite overwrapped cylinders with built-in mechanical preloads. The relaxation of preload in the composite is critical to the service life cycle of applications such as gun tubes and composite rotors, which are designed and built with a preload to achieve desired mechanical performance.

6. References

Chien, L. S., and J. T. Tzeng. "A Thermal Viscoelastic Analysis for Thick-Walled Composite Cylinders." *Journal of Composite Materials,* vol. 29, no. 4, pp. 525–548, 1995.

Christensen, R. M. *Theory of Viscoelasticity, An Introduction, 2nd edition.* New York: Academic Press, Inc., 1982.

Ferry, J. D. *Viscoelastic Properties of Polymer.* New York: John Wiley & Sons, Inc., 1961.

Hashin, Z. "Viscoelastic Behavior of Heterogeneous Media." *Journal of Applied Mechanics,* vol. 32, pp. 630–636, 1965.

Kim, R. Y., and J. T. Hartness. "Time-Dependent Response of AS-4/PEEK Composite." *Proceedings of the 19th International SAMPE Technical Conference*, pp. 468–475, October 1987.

Muki, R., and E. Sternberg. "On Transient Thermal Stresses in Viscoelastic Materials With Temperature-Dependent Properties." *Journal of Applied Mechanics,* pp. 193–207, 1961.

Rogers, T. G., and E. H. Lee. "The Cylinder Problem in Viscoelastic Stress Analysis." *Quarterly of Applied Mathematics,* vol. 22, pp. 117–131, 1964.

Schapery, R. A. "Application of Thermodynamics to Thermomechanical, Fracture, and Birefringent Phenomena in Viscoelastic Media." *Journal of Applied Physics,* vol. 35, no. 5, pp. 1451–1465, 1964.

Schapery, R. A. "Stress Analysis of Viscoelastic Composite Materials." *Journal of Composite Materials,* vol. 1, pp. 228–267, 1967.

Tzeng, J. T. "Viscoelastic Behavior of Composite Rotors at Elevated Temperatures." *IEEE Transactions of Magnetics,* vol. 33, no. 1, pp. 413–418, 1997.

Tzeng, J. T., and L. S. Chien. "A Thermal/Mechanical Model of Axially Loaded Thick-Walled Composite Cylinders." *Journal of Composites Engineering,* vol. 4, no. 2, pp. 219–232, 1994.

Williams, M. L. "Structural Analysis of Viscoelastic Materials." *AIAA Journal,* vol. 2, no. 5, pp. 785–808, 1964.

INTENTIONALLY LEFT BLANK.

NO. OF COPIES	ORGANIZATION
2	DEFENSE TECHNICAL INFORMATION CENTER DTIC DDA 8725 JOHN J KINGMAN RD STE 0944 FT BELVOIR VA 22060-6218
1	HQDA DAMO FDQ DENNIS SCHMIDT 400 ARMY PENTAGON WASHINGTON DC 20310-0460
1	DPTY ASSIST SCY FOR R&T SARD TT F MILTON RM 3EA79 THE PENTAGON WASHINGTON DC 20310-0103
1	OSD OUSD(A&T)/ODDDR&E(R) J LUPO THE PENTAGON WASHINGTON DC 20301-7100
1	CECOM SP & TRRSTRL COMMCTN DIV AMSEL RD ST MC M H SOICHER FT MONMOUTH NJ 07703-5203
1	PRIN DPTY FOR TCHNLGY HQ US ARMY MATCOM AMCDCG T M FISETTE 5001 EISENHOWER AVE ALEXANDRIA VA 22333-0001
1	PRIN DPTY FOR ACQUSTN HQS US ARMY MATCOM AMCDCG A D ADAMS 5001 EISENHOWER AVE ALEXANDRIA VA 22333-0001
1	DPTY CG FOR RDE HQS US ARMY MATCOM AMCRD BG BEAUCHAMP 5001 EISENHOWER AVE ALEXANDRIA VA 22333-0001

NO. OF COPIES	ORGANIZATION
1	INST FOR ADVNCD TCHNLGY THE UNIV OF TEXAS AT AUSTIN PO BOX 202797 AUSTIN TX 78720-2797
1	USAASA MOAS AI W PARRON 9325 GUNSTON RD STE N319 FT BELVOIR VA 22060-5582
1	CECOM PM GPS COL S YOUNG FT MONMOUTH NJ 07703
1	GPS JOINT PROG OFC DIR COL J CLAY 2435 VELA WAY STE 1613 LOS ANGELES AFB CA 90245-5500
1	ELECTRONIC SYS DIV DIR CECOM RDEC J NIEMELA FT MONMOUTH NJ 07703
3	DARPA L STOTTS J PENNELLA B KASPAR 3701 N FAIRFAX DR ARLINGTON VA 22203-1714
1	USAF SMC/CED DMA/JPO M ISON 2435 VELA WAY STE 1613 LOS ANGELES AFB CA 90245-5500
1	US MILITARY ACADEMY MATH SCI CTR OF EXCELLENCE DEPT OF MATHEMATICAL SCI MDN A MAJ DON ENGEN THAYER HALL WEST POINT NY 10996-1786
1	DIRECTOR US ARMY RESEARCH LAB AMSRL CS AL TP 2800 POWDER MILL RD ADELPHI MD 20783-1145

NO. OF COPIES	ORGANIZATION
1	DIRECTOR US ARMY RESEARCH LAB AMSRL CS AL TA 2800 POWDER MILL RD ADELPHI MD 20783-1145
3	DIRECTOR US ARMY RESEARCH LAB AMSRL CI LL 2800 POWDER MILL RD ADELPHI MD 20783-1145
	ABERDEEN PROVING GROUND
4	DIR USARL AMSRL CI LP (305)

NO. OF COPIES	ORGANIZATION
1	DFNS UCLEAR AGNCY INVTV CNCPTS DIV JYUJI D HEWITT 6801 TELEGRAPH RD ALEXANDRIA VA 22310-3398
2	PEO ARMAMENTS SFAE AR PM D ADAMS T MCWILLIAMS PICATINNY ARSENAL NJ 07806-5000
1	PEO FAS SFAE FAS PM H GOLDMAN PICATINNY ARSENAL NJ 07806-5000
4	PM CRUSADER G DELCOCO D ELLIS B MACHAK J SHIELDS PICATINNY ARSENAL NJ 07806-5000
2	PM SADARM SFAE FAS SD PICATINNY ARSENAL NJ 07806-5000
4	PM TMAS SFAE AR TMA COL BREGARD K KIMKER SFAE AR TMA MD K KOWALSKI SFAE AR TMA MS D GUZIEWICZ PICATINNY ARSENAL NJ 07806-5000
2	DIR USARL AMSRL SE L D SNIDER AMSRL SE L D WOODBURY 2800 POWDER MILL RD ADELPHI MD 20783

NO. OF COPIES	ORGANIZATION
1	CDR US ARMY ARDEC F MCLAUGHLIN PICATINNY ARSENAL NJ 07806-5000
1	CDR US ARMY ARDEC AMSMC PBM K PICATINNY ARSENAL NJ 07806-5000
2	CDR US ARMY ARDEC AMSTA AR CC J HEDDERICH COL SINCLAIR PICATINNY ARSENAL NJ 70806-5000
1	CDR US ARMY ARDEC AMSTA AR CCH J DELORENZO PICATINNY ARSENAL NJ 07806-5000
1	CDR US ARMY ARDEC AMSTA AR CCH P J LUTZ PICATINNY ARSENAL NJ 07806-5000
4	CDR US ARMY ARDEC AMSTA AR CCH T R CARR P CHRISTIAN N KRASNOW S MUSALLI PICATINNY ARSENAL NJ 07806-5000
1	CDR US ARMY ARDEC AMSTA AR CCH V E FENNELL PICATINNY ARSENAL NJ 07806-5000
2	CDR US ARMY ARDEC AMSTA AR FSA M D DEMELLA F DIORIO PICATINNY ARSENAL NJ 07806-5000

NO. OF COPIES	ORGANIZATION
3	CDR US ARMY ARDEC AMSTA AR TD V LINDNER T PRICE C SPINELLI PICATINNY ARSENAL NJ 07806-5000
1	CDR USA BELVOIR RD&E CTR STRBE JBC FORT BELVOIR VA 2200-5605
4	CDR US ARMY MICOM AMSMI RD W MCCORKLE AMSMI RD ST P DOYLE AMSMI RD ST CN T VANDIVER AMSMI RD ST WF M COLE REDSTONE ARSENAL AL 35898
3	CDR WATERVLIET ARS SMCWV QAE Q C HOWD SMCWV QA QS K INSCO SMCWV SPM T MCCLOSKEY B25 3 WATERVLIET NY 12189-4050
4	DIR ARO G ANDERSON J CHANDRA A CROWSON R SINGLETON PO BOX 12211 RESEARCH TRIANGLE PARK NC 27709-2211
9	DIR BENET LABS AMSTA AR CCB C KITCHENS J KEANE J BATTAGLIA J VASILAKIS G FRIAR V MONTVORI J WRZOCHALSKI R HASENBEIN AMSTA AR CCB R S SOPOK WATERVLIET NY 12189-4050

NO. OF COPIES	ORGANIZATION
1	DIR USA CRREL P DUTTA 72 LYME RD HANOVER NH 03755
2	DIR DARPA J KELLY B WILCOX 3701 N FAIRFAX DR ARLINGTON VA 22203-1714
1	EXPDTNRY WF DIV N85 F SHOUP 2000 NAVY PENTAGON WASHINGTON DC 20350-2000
2	OFC OF NAVAL RSCH MECH DIV CODE 1132SM Y RAJAPAKSE D SIEGEL 351 800 N QUINCY ST ARLINGTON VA 22217
1	DAVID TAYLOR RSCH CTR SHIP STRCTRS & PRTCTN DEPT J CORRADO CODE 1702 BETHESDA MD 20084
2	DAVID TAYLOR RSCH CTR R ROCKWELL W PHYILLAIER BETHESDA MD 20054-5000
1	NAVAL ORD STN ADVNCD SYS TECH BR D HOLMES CODE 2011 LOUISVILLE KY 40214-5245
1	CDR NSSC D LIESE 2531 JEFFERSON DVS HWY ARLINGTON VA 22242-5160
5	CDR NSWC CODE D4 M E LACY CODE G30 J H FRANCIS CODE G33 J FRAYSSE G GRAFF R HUBBARD 3 CP DAHLGREN VA 22448

NO. OF COPIES	ORGANIZATION
1	CDR NSWC CRANE DIV CODE 20HR M JOHNSON LOUISVILLE KY 40214-5245
2	CDR WRGHT PTRSN AFB WL FIV A MAYER WL MLBM S DONALDSON 2941 P STREET STE 1 DAYTON OH 45433
2	NASA LANGLEY RSCH CTR MS 266 AMSRL VS W ELBER AMSRL VS S F BARTLETT JR HAMPTON VA 23681-0001
1	ARGONNE NTNL LAB J M KRAMER 9700 SO CASS AVE ER 207 ARGONNA IL 60439-4841
1	BATTELLE M SMITH PO BOX 999 RICHLAND WA 99352
6	DIR LLNL R CHRISTENSEN S DETERESA W FENG A HOLT M FINGER F MAGNESS PO BOX 808 LIVERMORE CA 94550
1	OAK RIDGE NTNL LAB R M DAVIS PO BOX 2008 OAK RIDGE TN 37831-6195

NO. OF COPIES	ORGANIZATION
5	DIR SNL APLD MCHNCS DPT DIV 8241 G BENEDETTI D DAWSON W KAWAHARA P NIELAN K PERANO PO BOX 969 LIVERMORE CA 94550-0096
4	INST FOR ADVNCD TECH H FAIR T KIEHNE I MCNAB P SULLIVAN 4030 2 W BRAKER LN AUSTIN TX 78759
1	NASA LEWIS RESEARCH CTR C C CHAMIS 21000 BROOKPARK ROAD CLEVELAND OH 44135
1	NAVAL SEA SYSTEMS COMMAND GENE CAMPONESCHI NAVSEA 03 R11 2531 JEFFERSON DAVIS HWY ARLINGTON VA 22242-5160
1	DIR NIST PLYMR DIV PLYMRS RM A209 G MCKENNA GAITHERSBURG MD 20899
1	DIR NIST POLYMER DIVISION D HUNSTON BLDG 224 GAITHERSBURG MD 20899
1	DIR NIST BUILDING & FIRE RESEARCH LAB JOHNNIE CHIN GAITHERSBURG MD 20899
1	RENSSELAER POLY INST R B PIPES PITTSBURG BLDG TROY NY 12180-3590

NO. OF COPIES	ORGANIZATION
1	DREXEL UNIVERSITY ALBERT S D WANG 32ND & CHESTNUT STS PHILADELPHIA PA 19104
1	PURDUE UNIVERSITY SCHOOL OF AERO & ASTRO C T SUN W LAFAYETTE IN 47907-1282
2	STANFORD UNIVERSITY DEPT OF ARNTCS & AIRBLSTCS S TSAI G SPRINGER STNFORD CA 94305
2	UNIV OF ILLINOIS AT URBANA CHAMPAIGN NATL CTR FOR COMPOSITE MATERIALS RESEARCH H HILTON J ECONOMY 104 S WRIGHT ST URBANA IL 61801
1	UNIV OF KENTUCKY LYNN PENN 763 ANDERSON HALL LEXINGTON KY 40506-0046
1	UNIV OF UTAH MCHNCL & INDSTRL ENGRNG DEPT S SWANSON SALT LAKE CITY UT 84112
3	VIRGINIA POLY INST & ST UNIV DEPT OF ESM MICHAEL W HYER KENNETH L REIFSNIDER ALFRED LOOS BLACKSBURG VA 24061-0219
1	UNIV OF CA LA MANE DEPT ENGNRNG IV H T HAHN LOS ANGELES CA 90024-1597

NO. OF COPIES	ORGANIZATION
2	UNIV OF DAYTON RSCH INST R Y KIM A K ROY 300 COLLEGE PRK AVE DAYTON OH 45469-0168
1	UNIV OF DE CTR FOR CMPST MATLS J GILLESPE 201 SPENCER LAB NEWARK DE 19716
1	UNIV OF MD DEPT OF AEROSPC ENGNRNG A J VIZZINI COLLEGE PARK MD 20742
1	UNIV OF NY AT BUFFALO DEPT OF ELCTRCL ENGNRNG J SARJEANT BOX 601900 BUFFALO NY 14260-1900
4	UNIV OF TX AT AUSTIN CTR FOR ELCTRMCHNCS J KITZMILER J PRICE R TOMSON A WALLS 10100 BURNET RD AUSTIN TX 78758-4497
1	US MILITARY ACDMY DEPT OF CVL AND MCHNCL RSCH LABS J TROVILLION PO BOX 9005 CHAMPAIGN IL 61826-9005
1	AAI CORP TECH LIBRARY PO BOX 126 HUNT VALLEY MD 21030-0126
2	ADVNCD CMPST MATLS CORP R HOOD J RHODES 1525 S BUNCOMBE RD GREER SC 29651-9208

NO. OF COPIES	ORGANIZATION
3	ALLIANT TECHSYS INC J BODE C CANDLAND K WARD 5901 LINCOLN DR MINNEAPOLIS MN 55346-1674
1	ALLIANT TECHSYS INC T HOLMQUIST 600 SECOND ST NE HOPKINS MN 55343
1	AMOCO PRFRMNC PRODUCTS M MICHNO JR 4500 MCGINNIS FERRY RD ALPHARETTA GA 30202-3944
1	APPLIED COMPOSITES W GRISCH 333 NO SIXTH ST ST CHARLES IL 60174
1	BRUNSWICK DFNS T HARRIS 174 JFRSN DVS HWY STE 410 ARLINGTON VA 22202
1	CHAMBERLAIN MFG CORP R&D DIV M TOWNSEND 550 ESTHER ST WATERLOO IA 50704
1	CSTM ANLYTCL ENGRNG SYS INC A ALEXANDER STAR RT BOX 4A FLINTSTONE MD 21530
3	HERCULES INC R BOE J POESCH F POLICELLI PO BOX 98 MAGNA UT 84044

NO. OF COPIES	ORGANIZATION
3	HERCULES INC G KUEBELER B MANDERVILLE JR J VERMEYCHUK HERCULES PLZ WILMINGTON DE 19894
1	HEXCEL M SHELENDICH 11555 DUBLIN BLVD PO BOX 2312 DUBLIN CA 94568-0705
1	IAP RSCH INC A CHALLITA 2763 CULVER AVE DAYTON OH 45429
1	INTGRTD CMPST TECH H PERKINSON JR PO BOX 397 YORK NEW SALEM PA 17371-0397
1	INTERFEROMETRICS INC R LARRIVA VP 8150 LESSBURG PIKE VIENNA VA 22100
1	KAMAN SCNCS CORP T HAYDEN PO BOX 7463 COLORADO SPRINGS CO 80933
2	LORAL VOUGHT SYS K COOK G JACKSON 1701 W MARSHALL DR GRAND PRAIRIE TX 75051
2	MARTIN MARIETTA CORP P DEWAR L SPONAR 230 E GODDARD BLVD KING OF PRUSSIA PA 19406
1	NOESIS INC A BOUTZ 1500 WILSON BLVD STE 1224 ARLINGTON VA 22209

NO. OF COPIES	ORGANIZATION
2	PRIMEX TECH FLNCHBGH DIV E STEINER B STEWARD PO BOX 127 RED LION PA 17356
1	PRIMEX TECH L WHITMORE 10101 9TH ST NO ST PETERSBURG FL 33702

NO. OF COPIES	ORGANIZATION
	ABERDEEN PROVING GROUND
27	DIR USARL AMSRL WM, L JOHNSON J MCCAULEY D VIECHNICKI G HAGNAUER AMSRL WM P, A HORST E SCHMIDT AMSRL WM PB, P PLOSTINS AMSRL WM MB, J BENDER L BURTON B BURNS W DRYSDALE D GRANVILLE D HOPKINS D HENRY C HOPPEL R KASTE J TZENG A FRYDMAN B FINKS T BOGETTI AMSRL WM T, W F MORRISON AMSRL WM TA, W BRUCHEY W GILLICH AMSRL WM TC, R COATES W DE ROSSET AMSRL WM WA, B MOORE AMSRL WM WC , T HAUG

REPORT DOCUMENTATION PAGE

Form Approved
OMB No. 0704-0188

1. AGENCY USE ONLY *(Leave blank)*

2. REPORT DATE
January 1998

3. REPORT TYPE AND DATES COVERED
Final, Oct 95 - Dec 96

4. TITLE AND SUBTITLE
Viscoelastic Response of Prestressed Composite Cylinders for Rotating Machinery Applications

5. FUNDING NUMBERS
PR: 1L162618AH80

6. AUTHOR(S)
Jerome T. Tzeng

7. PERFORMING ORGANIZATION NAME(S) AND ADDRESS(ES)
U.S. Army Research Laboratory
ATTN: AMSRL-WM-MB
Aberdeen Proving Ground, MD 21005-5066

8. PERFORMING ORGANIZATION REPORT NUMBER
ARL-TR-1590

9. SPONSORING/MONITORING AGENCY NAMES(S) AND ADDRESS(ES)

10.SPONSORING/MONITORING AGENCY REPORT NUMBER

11. SUPPLEMENTARY NOTES

12a. DISTRIBUTION/AVAILABILITY STATEMENT
Approved for public release; distribution is unlimited.

12b. DISTRIBUTION CODE

13. ABSTRACT *(Maximum 200 words)*

Energy storage devices such as composite rotors are built with radial precompression to enhance mechanical performance; however, the preload might decrease due to the viscoelastic behavior of materials at elevated temperatures. In this investigation, an analytical solution is developed to study the viscoelastic problem of thick-walled cylinders. The analysis accounts for ply-by-ply variations of properties, fiber orientations, and temperature gradients through the thickness of cylinders. Fiber-reinforced composite materials generally illustrate extreme anisotropy in viscoelastic behavior. The viscoelasticity exists mainly in matrix-dominant properties such as transverse and shear while the fiber-dominant properties behave more like elastic mediums. Accordingly, the viscoelastic characteristics of composite cylinders are quite different from those of isotropic cylinders. Currently, finite-element packages such as ABAQUS, ANSYS, and DYNA3D are not suitable for the viscoelastic analysis of composite cylinders because of the lack of anisotropic viscoelastic elements. The prestress in the hoop-wound fibers, which generates radial compression in the cylinders, might decrease due to Poisson's effect alone from the creep behavior in the transverse properties of composite. The result also shows the effects of layup construction and fiber orientations on the anisotropic behavior of composite cylinders.

14. SUBJECT TERMS
composite, viscoelasticity, compulsator

15. NUMBER OF PAGES
35

16. PRICE CODE

17. SECURITY CLASSIFICATION OF REPORT	18. SECURITY CLASSIFICATION OF THIS PAGE	19. SECURITY CLASSIFICATION OF ABSTRACT	20. LIMITATION OF ABSTRACT
UNCLASSIFIED	UNCLASSIFIED	UNCLASSIFIED	UL

NSN 7540-01-280-5500

Standard Form 298 (Rev. 2-89)
Prescribed by ANSI Std. 239-18 298-102

INTENTIONALLY LEFT BLANK.

USER EVALUATION SHEET/CHANGE OF ADDRESS

This Laboratory undertakes a continuing effort to improve the quality of the reports it publishes. Your comments/answers to the items/questions below will aid us in our efforts.

1. ARL Report Number/Author ARL-TR-1590 (Tzeng) ________ Date of Report January 1998 ________

2. Date Report Received ________________________________

3. Does this report satisfy a need? (Comment on purpose, related project, or other area of interest for which the report will be used.) ________________________________

4. Specifically, how is the report being used? (Information source, design data, procedure, source of ideas, etc.) ________________________________

5. Has the information in this report led to any quantitative savings as far as man-hours or dollars saved, operating costs avoided, or efficiencies achieved, etc? If so, please elaborate. ________________________________

6. General Comments. What do you think should be changed to improve future reports? (Indicate changes to organization, technical content, format, etc.) ________________________________

CURRENT ADDRESS

Organization ________________________________

Name ________________ E-mail Name ________________

Street or P.O. Box No. ________________________________

City, State, Zip Code ________________________________

7. If indicating a Change of Address or Address Correction, please provide the Current or Correct address above and the Old or Incorrect address below.

OLD ADDRESS

Organization ________________________________

Name ________________________________

Street or P.O. Box No. ________________________________

City, State, Zip Code ________________________________

(Remove this sheet, fold as indicated, tape closed, and mail.)

(DO NOT STAPLE)